Wearable Sensor Based Stress Management Using Integrated Respiratory and ECG Waveforms

Kemeng Chen[1], Wolfgang Fink[1,2] and Janet Roveda[1]
Department of Electrical and Computer Engineering[1]
Department of Biomedical Engineering[2]
University of Arizona, Tucson, AZ 85721

Richard D. Lane[1,2], John Allen[1,2], and Johnny Vanuk[1]
Departments of Psychiatry[1] and Psychology[2]
University of Arizona, Tucson, AZ 85724[1], 85721[2]

***Abstract*—Wearable technology and mobile platforms are becoming more and more popular in health care. This paper introduces a real time stress management system using wearable sensors and Smartphone mobile platform. The new system estimates stress level in real time using heart rate variability and patient activity cycles, and provides relaxation exercises instantaneously to help manage stress. The system relies on a wearable sensor to collect data (i.e., heart rate and respiration rate) and transmits data to Smartphones using Bluetooth to further process data. We also introduce a new breathing template matching algorithm to identify the best breathing exercise for users. A 2D visualization display shows that stress can be effectively relieved by the proposed stress management system.**

Keywords— Stress management, Smartphone mobile platform, Stress relaxation program, Wearable technology

I. INTRODUCTION

Wearable technology has been widely used in clinical context such as disorder detection, treatment efficiency assessment, home rehabilitation and other healthcare research [1]. An important application is stress management. All people have experienced stress and some have been affected negatively in their daily life and health [1, 2, 3]. One key reason is the fact that the human body is designed to respond to challenges and threats with an orchestrated set of physiological responses that facilitate adaptive behaviors. These responses are mediated by a system that includes a network of nerves connecting the brain and body. One part of the nervous system that slows the heart rate is called the "vagus nerve". Activating the vagus nerve promotes a relaxation response [3]. It is possible to monitor vagus nerve activity using simple, inexpensive and readily available technology such as wearable technologies, mobile platforms and real time data driven tracking and management. This paper discusses how to use wearable technology and a mobile platform to monitor vagus nerve activity. We increase the vagus nerve activity when needed or as desired in order to promote relaxation and better health. Enabling vagus nerve activity has been found to be very useful in wound healing [4], post cardiovascular surgery recovery, and post-traumatic stress disorder [5]. One of our recent efforts [6] involves the development of such a stress management scheme that collects user data including heart rate and respiration rate, and transmits them to smart phones using Bluetooth to further process data. The stress management program estimates stress level based on heart rate variability and respiratory waveforms, and then provides relaxation exercises such as YOGA breathing trainings [7-10] to help manage stress.

The contributions of this paper includes: 1) a new stress management system that employs wearable sensors to collect heart rate and respiratory activities in real time; 2) an application on a mobile platform that integrates real time stress monitoring with relaxation exercises. We emphasize stress intervention through a relaxation program (i.e., breathing training) to form a feedback loop which can help users to lower their stress level. This new application can be executed in parallel without interrupting users' relaxation programs; 3) stress level estimation through heart rate variability (HRV) based on QRSTools [3, 11]; and 4) a new breathing pattern matching algorithm to find the optimal breathing exercise for users.

II. ARCHITECTURE OF THE STRESS MANAGEMENT SYSTEM

A. System architecture

Figure 1 describes the architecture of the new stress management system. At the front end, wearable sensors such as Zephyr sensor [12] provide measurements of patients' respiration rate, heart rate, body movements and other basic information. These wearable sensors are low power and can

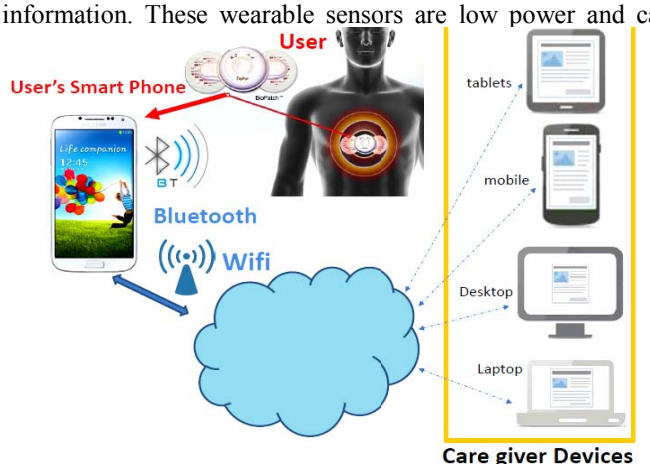

Fig 1. The architecture for the stress management system using wearable technology, smartphone mobile platform and cloud to establish real time stress monitoring and intervention.

978-1-4673-7201-5/15/$31.00 ©2015 IEEE

work over 24 hours without charging to create baseline measurements for patients. In our current system, the Smartphone accepts measurements from wearable sensors through Bluetooth communications. Equipped with multiple cores and wireless data links, Smartphones provide communications to local data centers through a wireless data link and enable basic data analysis capability locally on the Smartphones. The cloud offers data storage for users and real time data monitoring and analysis for health care providers. Text messages and warnings can be directly displayed on caregivers' smartphones through *software as a service* (SaaS).

Figure 2 shows the front end of the stress management system. We choose Zephyr BioPatch as the integrated wearable sensor node and Samsung Smartphone as our mobile platform. BioPatch has integrated accelerometer, ECG circuit and temperature sensor onto one chip. With two standard ECG electrodes, we can attach BioPatch onto users' chest. This BioPatch can measure users' heart rate, respiration rate, posture, activity and core temperature. We establish wireless communication between the BioPatch and the Samsung mobile phone via Bluetooth. Note that our stress management system is compatible with other wearable sensors and mobile platforms. We will further discuss the integrated wearable sensors in subsection B.

Fig. 2. The front end of the stress management system using Zephyr BioPatch [13] as the wearable sensor node and Samsung phone as the mobile platform.

Figure 3 displays the key software technologies used for this stress management system. For example, we use Android Operating system to create Application Program Interface (API) between the wearable sensor node and the Smartphone. On the cloud, various data analysis and mining approaches are exploited to provide reliable stress level estimation. For example, we provide a set of heart rate variability evaluations to detect and eliminate ECG noise. We also use QRS detection algorithms [3, 8] to analyze Heart Rate Variability (HRV). QRS refers to a combination of the three graphic deflections on an ECG waveform. Index equipped database storage on local data center will facilitate remote data management and search. To perform real time monitoring and intervention, we integrate basic data analysis and feature filtering in an app that can be executed directly on the mobile platforms. For example, we use Root Mean Square of Successive Difference (RMSSD) [14] to assess HRV. The Successive difference between interbeat intervals reflects how the timing of each beat is changing dynamically, attributable in large part to vagal influence. By taking the RMS of these successive differences, higher values reflect greater beat-to-beat variability, summarized by this computationally-efficient metric. We estimate RMSSD at the mobile platform, e.g., the Samsung phone in Figure 2. Other more computationally intensive metrics can be derived using remote computers and services.

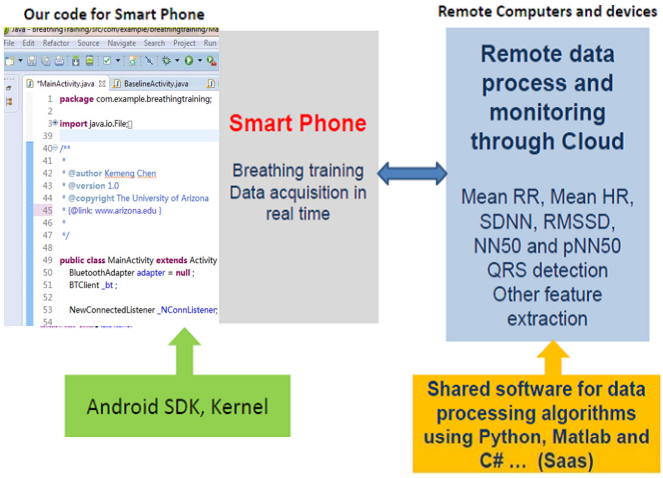

Fig 3. Key software support technologies used in the new stress management system development.

An app is situated on a mobile platform to perform front end real time stress management. Figure 4 demonstrates the basic diagram of this app. First we receive a data stream from the wearable sensor node. Then we perform RMSSD computation on the Smartphone. A RMSSD threshold is setup for each user based on one's baseline assessment. This threshold is used to identify whether one is stressed or not. If the user is identified as "Stressed", we activate a breathing pattern matching algorithm to identify the optimal breathing exercise for the user based on his/her respiratory waveform. If the user's stress level drops to normal, the exercise will stop and real time HRV monitoring continues. We refer to this whole monitoring and exercising procedure as "stress intervention". While there are many breathing exercises, without the loss of generality, this paper focuses on YOGA [7] breathing exercises as an example for stress intervention. Studies have shown that low HRV is an indication of high stress level [2]. And breathing exercise can help user increase HRV and relieve stress [7-10].

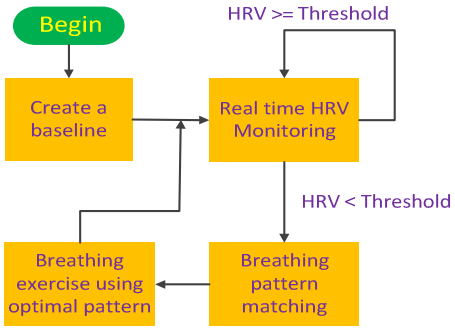

Fig 4. Block diagram of the proposed real time stress management System.

B. *Design Integrated Wearable Sensor Node*

Wearable sensors stream real time data to mobile platforms via low-power and reliable wireless interfaces. Without interrupting users' daily life, we expect these sensors to work

978-1-4673-7201-5/15/$31.00 ©2015 IEEE

continuously for hours or days. In addition to the long working hours, we also design wearable sensors to have high data acquisition rate. In the current stress management system, we use 1000Hz for ECG sensor sampling frequency with each sample represented as 10 bits for transmission and 12 bits binary for storage. Instead of using distributed body sensors, we choose the integrated wearable ones. Use BioPatch [13] as an example. It integrates ECG sensor, accelerometer, and temperature sensor onto one chip. This integration allows simplification of individual sensor design. For example, instead of designing a separate sensor for respiration rate, one can implement impedance pneumography by using the signal passing through the same electrodes of the ECG sensor. Hence, by wearing one integrated wearable sensor node, we can measure heart rate, respiration rate, posture, activity and core temperature.

Battery life and weight are also important features for wearable sensors. Most integrated wearable sensor nodes use an internal lithium cell battery. Different data transmitting modes can affect battery life by over 30%. Use BioPatch as an example. Data packets record sensory data into flits. Each flit contains a header that specifies the type and the size of the data. Signals such as ECG, respiratory waveform, posture, temperature, etc. are stored as packets. The integrated wearable sensor node transmits one packet to a mobile platform per second. The size of the data packet is determined by each sensor's sampling rate. By using low sampling rate for slow change signals such as body temperature, the data packet size may be reduced which in turn reduces packet transmission time and power consumption during data transmission.

C. *QRS detection and Heart Rate Variability for off-line calibration*

Because HRV is employed to assess stress level, it is important to calibrate the HRV estimation. HRV can be evaluated by using R to R peak intervals in ECG signal. Figure 5 shows QRS complex and R to R peak intervals. It displays two QRSs and the interval between the two R peaks is the R to R interval.

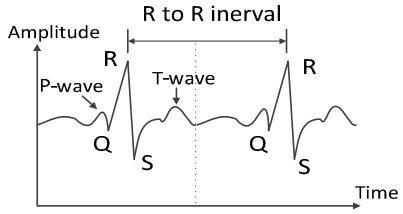

Fig 5. QRS complex and R to R interval on ECG signal.

We use RMSSD value to evaluate the changes between the two R peaks (i.e., interbeat intervals) over time. Computation of RMSSD follows the root mean square of successive difference.

$$RMSSD = \sqrt{\frac{1}{N-1}\left(\sum_{i=1}^{N-1}\left((R_{i+1}-R_i)-(R_i-R_{i-1})\right)^2\right)} \qquad (1)$$

where N is the number of R to R peak samples within a time window.

In the stress management system, we acquire raw ECG signals from the integrated wearable sensor node. We use accurate QRS detection algorithms to assure reliable HRV estimation. This step is also performed off-line to calibrate the HRV estimation for the real time stress management system. Automatic QRS complex detection is still a difficult task due to muscle movement, power line inference, and electrode artifacts from motion and high P or T-wave [3]. Many research efforts have focused on the QRS complex recognition. We choose QRSTool [3, 11] as our off-line calibration tool for the HRV estimation. Developed by Prof. John Allen (one of the co-authors of this paper) and his research group, QRSTool employs a peri-beat average QRS complex detection algorithm. The algorithm generates an average beat template and applies this template to the rest of ECG to identify other QRS complexes. In order to obtain a good average beat template, the QRSTool allows manual modification of beat detection to insert missing beats or delete redundant beats. The QRSTool first uses a hard threshold for a number of successive beats (e.g., 30 seconds long ECG) to detect the QRS complex given that change from baseline would not affect ECG within a short period of time. Based on these detected QRS complexes (beats), the algorithm can extract each individual heart beat based on pre- and post-beat length (80ms to 250ms) and then estimates an average prototype beat vector. Next, the algorithm filters the entire ECG waveform and generates another feature series. Finally, the R spikes can be extracted from the feature series.

In addition to the automatic detection of the QRS complex, how to improve the robustness of the detection algorithm and how to assess the respiratory-linked HRV are two main challenges that directly affect the success of the stress management system. For instance, tapping or brushing the user's chest area introduces high magnitude noise in the QRS complexes. In general, artifacts in the detection of R-R intervals can result in an invalid HRV [15]. QRSTool [3, 11] allows hand-corrected detection algorithms for artifacts to improvement the robustness of the detection algorithm. While we use the RMSSD value to assess stress level to activate YOGA breathing exercise, this paced intentional breathing also introduces changes in the various performance metrics we use to assess vagal control. In the current stress management system, we create baseline HRV measurement when the user is under spontaneous conditions. Thus, his/her breathing becomes a key indicator that allows us to discover the vagal system impact on variability in cardiac rate.

III. MATCH BREATHING EXERCISE PATTERN

Breathing exercises have been shown to be an effective way to relieve stress and help people calm down [3, 7-10]. During the breathing exercise, the user is required to breathe strictly following one selected exercise. One popular type of breathing exercise is referred to as YOGA exercise. Figure 6 shows four different YOGA breathing exercises. To illustrate the differences among these YOGA exercises, let us first introduce the concept of breathing pattern. A breathing pattern has three components: inhalation, hold, and exhalation. One

978-1-4673-7201-5/15/$31.00 ©2015 IEEE

breathing cycle is defined as a repeated, complete breathing template. Now, let us use the breathing pattern definition to introduce YOGA breathing exercises. Figure 6 (a) is a 4-4-6 pattern [7] which means that inhale time, hold time, and exhale time are 4 seconds, 4 seconds and 6 seconds respectively.

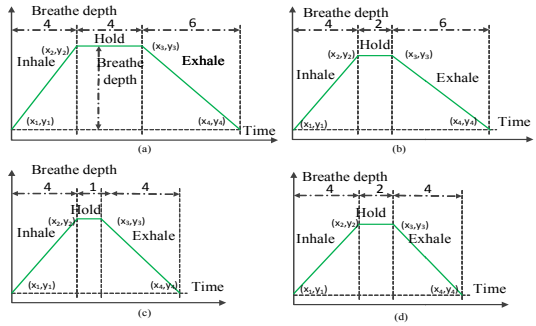

Fig 6. Four YOGA breathing exercises represented in trapezoidal.

The horizontal axis represents the time, and the vertical axis is the breathing depth. The other three YOGA exercises in Figure 6 (b) to (d) show the 4-2-6 pattern [8, 9], 4-1-4 pattern [10], and 4-2-4 pattern [10]. All YOGA exercises can be represented as trapezoidal waveforms. Note that different YOGA exercises can have diverse length in time and breathing depth. We refer to each user/patient as one test subject. It is important to notice that each test subject doing the same YOGA exercise may lead to different breathing depth and slopes of the respiratory waveforms. If two test subjects closely follow the same YOGA exercise, the only things in common in their respiratory waveforms may be the inhale time, the hold time and exhale time. We intend to identify the best breathing exercise for the test subject such that its inhale time, hold time and exhale time is very similar to the test subject's respiratory waveform.

A. Identify cycles for respiratory waveforms

The various uncertainties during the measurement and the high sensitivity of the wearable sensors are the leading causes of the noise occurring in the respiratory waveforms. Figure 7 shows a raw respiratory waveform with noise (i.e., circled locations in the Figure). Here, the horizontal axis represents the time in seconds. The vertical axis represents the breathing depth. From observation, each peak represents one breathing cycle. The raw respiratory waveform in Figure 7 has fourteen breathing cycles. However, due to the various noises with different amplitude and frequencies in the raw data, it is not trivial to identify cycles by directly searching for peaks and valleys in the time domain.

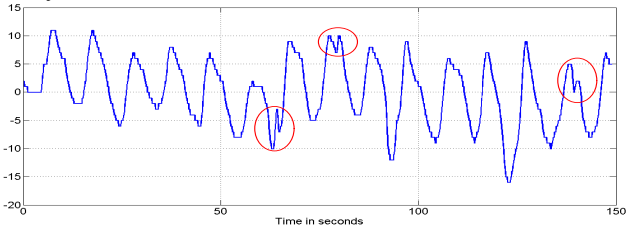

Fig 7. Noisy, raw respiratory waveforms with fourteen cycles in the time domain.

Therefore, we transform the time domain waveform to the frequency domain using Fourier transform after subtracting the mean of raw waveform to remove DC part. This is important as the mean of raw waveform represents the DC offset of data. DC offset is also regarded as the zero frequency component. This DC offset of raw respiratory waveform is several orders of magnitude higher than other frequency coefficients. In general, the design of sensor determines the DC component. In this case, as we use impedance pnenmography to detect respiration rate and generate respiratory waveform, the DC response of the user's chest area and electrode decides the DC component. In order to ensure the accuracy of other frequency coefficients, we remove the DC component by subtracting the mean of raw waveform. Without the loss of generality, we assume that any raw respiratory waveform is a combination of clean waveform with noise. In most cases, we assume that the occurring noises are additive ones, and are less significant than the clean waveform without noise. Figure 8 displays the single-sided frequency spectrum from 0 to π. The left top plot shows frequency coefficients of a raw respiratory waveform. The right top plot is a zoom-in view of range from 0 to $\pi/10$. The left bottom plot demonstrates the frequency coefficients after only preserving the ten most significant coefficients. The right bottom figure is a zoom-in view of the left bottom plot ranging from 0 to $\pi/10$. As shown in the left top figure in Figure 8, the magnitude of the frequency coefficients drops very fast from the large coefficients to the small ones. This means that a very small portion of coefficients (most significant coefficients) are a lot more significant than the rest. Therefore, we can remove the noise in the frequency domain by keeping only the most significant coefficients. In this case, we only keep the leading ten most significant coefficients.

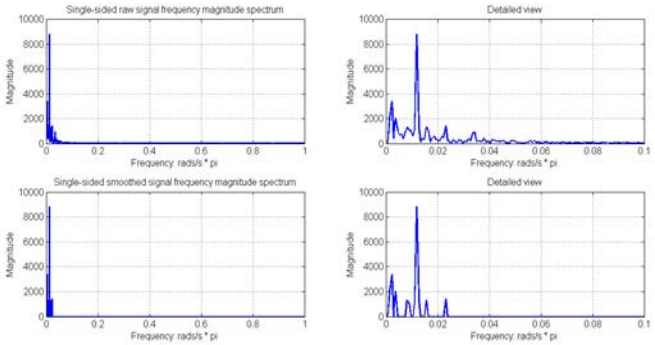

Fig 8. Single-sided frequency spectrum.

Figure 9 displays the Inverse Fourier Transform result using the ten most significant coefficients. We compare the processed waveform with the original raw respiratory one (the green colored waveform in Figure 9). Obviously, the blue waveform matches with the green one with little noise. Now, we can identify the breathing cycle using the processed waveform. By locating the valleys in the smoothed waveform, we can find the starting point and the end point of each cycle. This is the key idea of our new valley detection algorithm since noise and defects have been removed in the newly processed waveform.

978-1-4673-7201-5/15/$31.00 ©2015 IEEE

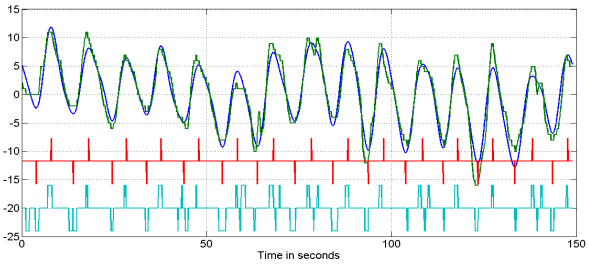

Fig 9. Breathing cycle detection results using the IFFT processed waveform and the original raw respiratory waveform.

To explain this whole procedure in a formal way, assume that $S=\{s_1, s_2 \cdots\cdots s_n\}$ represents a group of sample points in the time domain of the processed waveform. Then, any s_i $(i \in (2,n-1))$ that satisfies $(s_i<s_{i+1}$ AND $s_i<s_{i-1})$ is identified as a valley. A similar idea can be applied to identify peaks in the processed waveform. Figure 9 (plots at lower part of the figure) displays the results of the identified breathing cycles (in red). Vertical lines represent the valleys' and peaks' occurring time. One breathing cycle can be identified by two vertical, pointing downward lines. We also applied the same detection algorithm on the original raw respiratory waveform. Due to noises, the resulting indications of valleys and peaks are mixed with noise-caused valleys and noise-caused peaks (in light green). We therefore use the smoothed waveform to mark the starting and the ending point of each cycle and use those marks to extract breathing cycles from the raw respiratory waveform.

B. Identify inhale time, hold time, and exhale time for the original raw respiratory waveform

This section discusses how to find the inhale time, the hold time, and the exhale time given several different cycles of raw respiratory waveforms. Due to the variations in each cycle of the raw waveform, we compute the average of a set of respiratory waveforms cycles from raw data to get the mean respiratory waveform. As a first step, we perform left-side alignment for a group of cycles of the raw respiratory waveform so we always start with the beginning of an inhale cycle. Figure 10 displays the average respiratory waveform (in red) with the upper bound (in blue) and the lower bound (in green) derived from standard deviations. The variations mainly affect the breathing depth but have little influence on the inhale time, the hold time and the exhale time. Thus, we can conclude that by using an average respiratory waveform, we can identify accurate inhale, hold, and exhale times. Because the YOGA breathing exercises can be represented as four (or more) different trapezoidal waveforms, we propose to find one trapezoidal waveform that fits the average respiratory waveform in an "optimal" way (i.e., with minimum error).

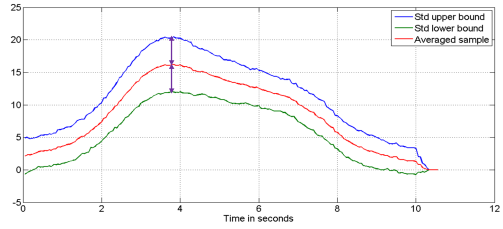

Fig 10. Averaged respiratory waveform with upper bound and lower bound.

There are two ways to achieve minimum error: minimizing L2-norm to get the overall error, or minimizing the maximum error. The following equations show the L2-norm method (2) and the min-max error approach (3).

$$\min\left(\sum_{i=1}^{N}(S_i - D_i)^2\right) \quad (2)$$

$$\min\left(\max_{i\in\{1\cdots N\}}\left(|S_i - D_i|\right)\right) \quad (3)$$

Each S_i is a data point in the average respiratory waveform. And D_i is a data point in one trapezoidal waveform. The end results of the above two equations are the optimal trapezoidal waveform that can have the least error. The proposed algorithm uses four representative points to represent a trapezoidal waveform: (x_1, y_1), (x_2, y_2), (x_3, y_3), and (x_4, y_4). The first and second points determine the inhale time; the second and third points determine the hold time; and the third and fourth points determine the exhale time. Note that the first and fourth points should have the same height which means $y_1 = y_4$ and so do the second and third points.

We compared performance of the two error minimization algorithms. The L2-norm based error minimization approach outperforms the min-max error algorithm. Firstly, degeneracy situations may occur in min-max error approach when two trapezoidal waveforms share the same maximum error value at different locations of the original raw waveforms. Instead of focusing on the maximum error, the L2-norm minimization method sums up all the errors occurring at different locations of the waveforms. It is therefore unlikely that two different trapezoidal waveforms may have the same minimum error in L2-norm. In addition to the degeneracy issue, potential alignment errors may also affect the outcome of the error minimization procedure. To illustrate, the test subject may not finish the exhale action completely before his/her next breathing cycle. This will lead to errors at the starting point and the end point. The type of errors will not cause major issues when we use L2-norm based error minimization as it sums up all errors in the form of $(S_i - D_i)^2$. The errors occurring at the beginning and the end point of each cycle only contribute to two error values in this summation. However, if such type of errors happen to be the maximum $|(S_i - D_i)|$, then the outcome of min-max error will be affected.

IV. IMPLEMENTATION AND EXPERIMENTAL RESULTS

The proposed stress management system has been implemented on Android OS 4.3 on Samsung Galaxy III version using JAVA and Android SDK. Zephyr BioPatch 3.0 is selected as the integrated wearable sensor nodes. Our sensor collects ECG at 1000 Hz, respiratory waveform at 18 Hz, together with other signals. It is equipped with Bluetooth working at 2.4 to 2.83 GHz. Data packet uses the standard RIFF format and packet transmission rate is 1 second. The battery life is approximately 22 hours with Bluetooth wireless communication. The algorithm to find best fitting breathing exercise has been implemented using MATLAB and tested off-line using real respiratory waveform recorded from our stress management system during user's breathing exercise.

978-1-4673-7201-5/15/$31.00 ©2015 IEEE

Figure 11 shows the L2-norm minimization result compared with the average respiratory waveform. The blue plot is the averaged waveform computed from the smoothed waveform cycles. And the green plot is the best trapezoidal waveform with minimum L2-norm error. X-axis for the four representative points is 2, 63, 87, and 181 respectively. Since our sensor works at fixed sampling rate, we can compute the inhale time, the hold time, and the exhale time using the four points. For example, the inhale time can be computed as $(x_2 - x_1)/fs$ = 3.38s. The hold time can be estimated as $(x_3 - x_2)/fs$ = 1.33s. And the exhale time is $(x_4 - x_3)/fs$ = 5.22s. We also map the time duration of the three breathing time into a three dimensional vector space and find the minimum Euclidean distance between the best trapezoidal waveform and the four YOGA exercises. Figure 12 shows the mapping results and the Euclidean distance (fs = 18 Hz). The three red lines are used to help identify the position of the red square which is the mapping of the average respiratory waveform cycle. YOGA exercise 4-2-6 with Euclidean distance 1.2 is the closest to the average respiratory waveform.

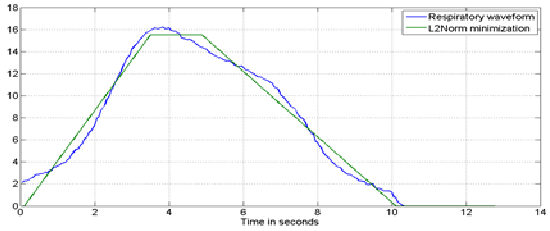

Fig 11. Optimal trapezoidal waveform using L2-norm error minimization.

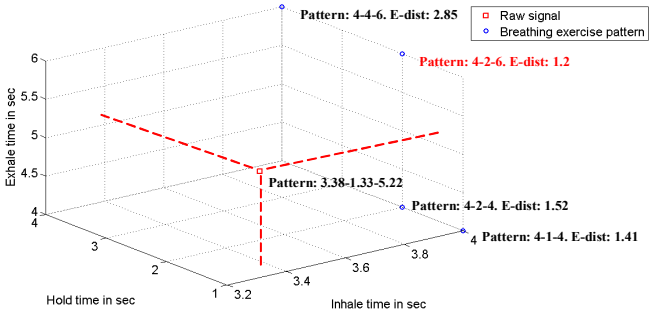

Fig 12. Identify the best YOGA exercise using Euclidian distance. Red square is the mapping of averaged waveform of raw signal and blue circles are four breathing exercise patterns. Each pattern contains its inhale, hold, and exhale time duration followed by Euclidean distance to the red square.

In addition, we also introduce a 2D color visualization to show the stress change when a test subject is using our stress management system. Figure 13 shows the color map of the stress level changes. Vertical axis is the breathing waveform from stage 1 to stage 3. Horizontal axis is the time axis where each unit is the time duration of a complete breathing cycle. Red color means a high stress level and yellow color indicates a moderate level of stress. Blue color defines a healthy state with low level stress. These stress levels are computed from HRV following equation (4). T_{stress} and $T_{relaxed}$ are two thresholds which determine the stress level based on HRV. Figure 13 shows that the test subject is under high level stress

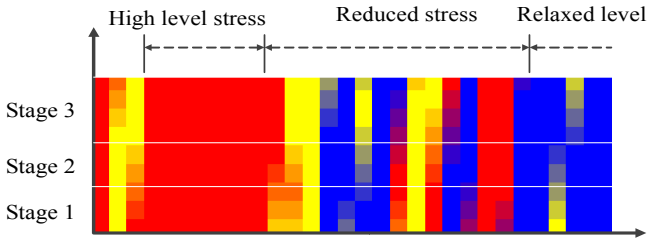

Fig 13. 2D visualization of stress level management.

$$color = \begin{cases} red\,(if\,(HRV \le T_{stress})) \\ yellow\,(if\,(T_{stress} < HRV \le T_{relaxed})) \\ blue\,(if\,(T_{relaxed} < HRV)) \end{cases} \quad (4)$$

during the labeled "High stress level" period on the left side. We observe that the red color occupies a large portion on the left side. Then, the stress level starts to decrease around the middle point along the horizontal axis during the labeled "Reduced stress" period where the color map starts to display a mixed color of yellow and blue. Finally, the stress level drops to a healthy level during the"Relaxed level" period. This 2D color visiualization can help users to directly "see" how their stress level changes when they follow the YOGA breathing exercises.

REFERENCES

[1] Shyamal Patel, Hyung Park, Paolo Bonato, Leighton Chan, Mary Rodgers, "A review of wearable sensors and systems with application in rehabilitation". Journal of NeuroEngineering and Rehabilitation. 9:21, 2012.

[2] J. Taelman, S. Vandeput, A. Spaepen, S. Van Huffel, "Influence of Mental Stress on Heart Rate and Heart Rate Variability". ECIFMBE 2008, IFMBE Proceedings 22, pp. 1366–1369, 2008.

[3] Allen, J.J.B., Chambers, A.S., & Towers, D.N., "The many metrics of cardiac chronotropy: A pragmatic primer and a brief comparison of metrics". Biological Psychology. 74, pp. 243-262, 2007

[4] Kristina Soon, Clare Acton, "Pain–induced stress: a barrier to wound healing". Clinic review, Wounds, UK. Vol. 2, No. 4, pp. 92-101, 2006.

[5] R. E. Pecoraro, G. E. Reiber, and E. M. Burgess, "Pathways to diabetic limb amputation. Basis for prevention". Diabetes Care. Vol. 13, No. 5, pp. 513- 521, 1990.

[6] UA15-018, Provisional Patent, "Real-time Vagal Monitoring and Intervention", Richard Lane, Janet M. Roveda, and John Allan.

[7] Brown, R. & Gerbarg, P., "The Healing Power of the Breath: Simple Techniques to Reduce Stress and Anxiety, Enhance Concentration, and Balance Your Emotions". Shambhala Publications. 2012, pp: 144-148.

[8] Calm Technique, Center for Clinical Interventions. Available: http://www.cci.health.wa.gov.au/docs/ACFA28D.pdf.

[9] Calm Technique, Center for Clinical Interventions. Available: http://www.cci.health.wa.gov.au/docs/Panic-11_Calming Technique.pdf.

[10] CALM BREATHING. AnxietyBC. Available at: http://www.anxietybc.com/sites/default/files/CalmBreathing.pdf

[11] Allen J.J.B., "Calculating metrics of cardiac chronotropy: A pragmatic overview". Psychophysiology, 39, S18, 2002.

[12] http://zephyranywhere.com/

[13] BioHarness™ 3 Logging System Interface. 2011. Zephyr Techonology.

[14] Von Neuman, J., Kent, R. H. , Bellinson, H.R., Hart, B. I., The mean square successive difference. The annuals of Mathematics and Statistics, 12, pp. 153-162, 1941.

[15] Berntson, G, Stowell, JR."ECG artificats and heart period variability: don't miss a beat", Psychophysiology, 35(1), pp:127-132, 1998.

978-1-4673-7201-5/15/$31.00 ©2015 IEEE